SDRP Journal of Nanotechnology & Material Science (ISSN: 2574-1888)

In vitro cytotoxicity studies on galactosylated chitosan nanoparticles for the delivery of oridonin to liver

DOI: 10.25177/JNMS.2.1.RA.410

Research

Received Date: 02nd Oct 2018
Accepted Date: 07th Dec 2018
Published Date:17th Dec 2018

Copy rights: © This is an Open access article distributed under the terms of International License.

Dandan Zheng[1], Chanmei Lv[2], Ran Zhang[3], Jinglong Wang[1,*]

[1] College of Food Science and Pharmaceutical Engineering, Zaozhuang University, Zaozhuang 277160, China.

[2] Department of pharmacy, Yantai Affiliated Hospital of Binzhou Medical University, Yantai 256603, China.

[3] Department of pharmacy, Middle District People's Hospital of the City, Zaozhuang 277100, China.

CORRESPONDENCE AUTHOR
Jinglong Wang
E-mail: jlwang8121@163.com
Tel: 0632-3786871; Fax: 0632-3786871

CITATION
Jinglong Wang, In vitro cytotoxicity studies on galactosylated chitosan nanoparticles for the delivery of oridonin to liver(2018)SDRP Journal of Nanotechnology & Material Science 2(1)

ABSTRACT

The objective of this study was to evaluate the *in vitro* antitumor activity of oridonin (ORI)-loaded nanoparticles decorated with galactosylated chitosan (ORI-GC-NP) aiming to overcome the poor specificity of oridonin for chemotherapy of hepatocellular carcinoma. In this research, ORI-GC-NP was prepared and characterized firstly. The average particle sizes of resultant nanoparticles were 247.2 nm. Then the cytotoxicity of blank nanoparticles without oridonin was determined to exclude the interference of excipients. Moreover, 3-(4,5-dimethylthiazol-2-yl) -2,5-diphenyltetrazolium bromide (MTT) assay and the observation of cell morphology were performed to determine the *in vitro* cytotoxicity against HepG2 cells (liver hepatocellular cells), with MCF-7 cell (human breast adenocarcinoma cell line) as control. Parallelly, ORI solutions and undecorated ORI nano particles (ORI-NP) were studied. The results suggested that the antitumor activities of the three formulations increased in a concentration and time dependent manner, and ORI-GC-NP showed higher inhibition rates against HepG2 cells compared to ORI solutions and ORI-NP. In regard of the cell lines, the cytotoxicity of ORI-GC-NP against HepG2 was higher than MCF-7 cells, indicating an increased specificity of ORI to hepatocellular carcinoma. In a conclusion, the overall results support the potential applications of galactosylated chitosan nanoparticles for hepatocyte-targeted delivery of ORI.

Keywords: *oridonin nanoparticles; galactosylated chitosan; in vitro; cytotoxicity; HepG2 cells*

INTRODUCTION

It has been reported that about 600 thousand patients worldwide suffer from HCC (hepatocellular carcinoma) annually, one of the most common and lethal malignancies [1, 2]. Oridonin (Figure 1), a diterpenoid compound, was gradually used as a chemotherapeutic

agent against liver cancers [3, 4], but limited for its poor specificity.

To overcome the limitations, the passive targeting and active targeting could be combined using galactosylated chitosan nanoparticles as the hepatocyte-targeted drug delivery system[5, 6]. Recently, the polymers of galactosylated chitosan (GC) were usually modified by conjuncting lactobionic acid to C2-amino groups of chitosan[7]. And then, the positively charged GC adhered to the negatively charged lipid nanoparticles through attractive ionic interaction [8, 9]. Active targeting of the polymeric nanoparticles to hepatocellular carcinoma cells was achieved by receptor-mediated endocytosis as the asialoglycoprotein receptor (ASGP-R) over-expressed on the surface of these tumor cells [10]. Additionally, the passive targeting of the nanoparticles varying in size from 100 to 600 nm depended on the enhanced permeability and retention (EPR) effect, which could promote selective passage of drugs through biological barriers [11-14].

Accordingly, nanoparticles modified with galactose residues were designed to enhance the targeting of oridonin to HCC cells. Oridonin-loaded nanoparticles coated with galactosylated chitosan were obtained and characterized through the measurement of particle size, and the *in vitro* antitumor activity in HepG2 cells was investigated in comparison with uncoated nanoparticles and oridonin solution formulation.

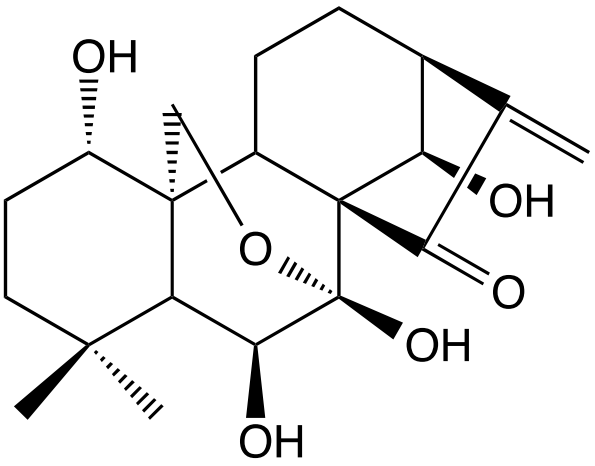

Figure 1. The chemical structure of oridonin.

MATERIALS AND METHODS

Materials

Oridonin (ORI) with the purity of 98%, was provided by Nanjing Zelang Pharmaceutical Co., Ltd. Galactosylated chitosan (GC) with a degree of substitution of galactose as 39% was synthesized in our lab previously. Dimethyl sulfoxide (DMSO) was provided by Sangon Biotech (Shanghai) Co., Ltd. Fetal bovine serum (Characterized FBS) was obtained from Tianjin Hao Yang Biological Technology Co., Ltd. Dulbecco's Modification of Eagle's Medium (DMEM) was bought from Invitrogen (USA). Penicillin-Streptomycin Solution (100×) was purchased from Beijing Solarbio Science & Technology Co., Ltd. MTT and trypsin were provided by Sigma (St. Louis, MO, USA). Water used in this study was purified by distillation, deionization and reverse osmosis (Milli-Q plus; Millipore, Billerica, MA). Other chemicals and solvents were of chromatographic and pharmaceutical grade.

Preparation and characterization of ORI-GC-NP

The GC-coated and uncoated nanoparticles, calling ORI-GC-NP and ORI-NP for short, were prepared as follows. Briefly, ORI was dispersed into 125 mg of medium chain triglyceride (MCT) and 1.75 mL of 120 mg/mL alcoholic lecithin solution, followed by adding 0.75 mL of acetone. This organic phase was subsequently mixed dropwise with 10 mL of 0.25 mg/mL GC aqueous solution under magnetic stirring. Afterwards, acetone, ethanol and a portion of water in the preparation were removed on a rotary evaporator under vacuum [8]. An identical protocol was then used to prepare ORI-NP without GC in the aqueous phase. The average particle sizes of ORI-GC-NP and ORI-NP were measured by the dynamic light scattering (DLS) method using a particle analyzer (Delsa^{TM} Nano C Particle Analyzer, Beckman Counter Ltd., USA). The morphology of NPs was investigated by transmission election microscope (TEM, Hitachi, Japan). To have a suitable testing concentration the samples were diluted with distilled water.

In vitro drug release profiles

The *in vitro* drug release property was determined in phosphate buffer saline (PBS, pH 7.4 and 6.0). The ORI-GC-NP (containing 10 mg oridonin) was transferred to a dialysis membrane bag (molecular cut-off = 12 kDa) and immersed fully in 200 mL of the release medium (37℃, 100 rpm). At predetermined time intervals, 2 mL of the release medium was withdrawn and replaced with an equal volume of fresh release medium. The amount of ORI was finally determined using a high performance liquid chromatography (HPLC, Agilent 100 series, USA) method: Injected volume: 20 μL; Hypersil-ODS_2 column (4.60 mm × 250 mm, 5 μm); mobile phase: water and methanol (45:55, v/v); elution rate: 1.0 mL/min; wavelength: 238 nm.

Cell line and cell culture

Human Hepatocellular Carcinoma Cell Line (HepG2 cells) and Michigan Cancer Foundation-7 (MCF-7 cells) were cultured in DMEM containing 10% fetal bovine serum, 100 U/mL of penicillin and 100 μg/mL of streptomycin. The cells were maintained at 37℃ in a humidified incubator with an atmosphere of 5% CO_2. For the two types of cancer cells, the medium was exchanged every day and the cells were subcultured every 2–3 days.

Cytotoxicity assay of blank nanoparticles

The cytotoxicity of blank nanoparticles without oridonin was determined firstly by MTT assay. HepG2 and MCF-7 cells in logarithmic growth phase were seeded at a density of 3.5×10^4 cells per well in 100 μL of the same medium for 12 h in 96-well plates before used. Then the cells were incubated with blank nanoparticles solution at various concentrations for 72 h. Subsequently, the media was removed and cells were washed with culture media. 200 μL serum-free culture media with 20 μL MTT (5 mg/mL) was then added to each well. After being incubated for an additional 4 h, the medium in plates were replaced with 150 μL DMSO. To dissolve the reacted dye, solutions were vigorously mixed. Optical density (OD) was subsequently read at 570 nm on a Microplate Reader with 630 nm as a reference wavelength. The cell viability rate was determined as follows: viability rate (%) = $OD_{\text{treated cells}} / OD_{\text{control cells}} \times 100\%$ [15]. Six samples of each assay were done parallelly.

In vitro antitumor activity test of drug-loaded nanoparticles

MTT assay was used to test the *in vitro* antitumor activity of oridonin loaded nanoparticles by the same method as the cytotoxicity assay of blank nanoparticles, while the blank nanoparticles were replaced by ORI-GC-NP, ORI-NP or ORI solution. In addition, the cell inhibitory rate was as follows: inhibitory rate (%) = $(OD_{\text{control cells}} - OD_{\text{treated cells}}) / OD_{\text{control cells}} \times 100\%$ [15]. IC_{50}, defined as the drug concentration required to inhibiting growth by 50% relative to controls, was used to express the cytotoxicity of drug-loaded nanoparticles.

Observation of cell morphology

HepG2 and MCF-7 cells were seeded overnight in 6-well plates and then treated with 54.88 μM of ORI-GC-NP, ORI-NP or ORI solution for 24 h. Subsequently, the cellular morphologies were estimated using a reverse fluorescence microscopy (Olympus, Japan).

RESULTS AND DISCUSSION

Characterization of ORI-loaded nanoparticles

From Figure 2, the sizes and morphologies of drug-loaded nanoparticles were exhibited, showing a unimodal and relatively narrow particle size distribution of the particles. The mean particle diameter of ORI-NP and ORI-GC-NP were 197.4 ± 5.9 nm (polydispersity index (PI) = 0.160 ± 0.008) and 247.2 ± 6.4 nm (PI = 0.276 ± 0.012), respectively. It could be observed in Figure 2-C that ORI-GC-NP presented a spherical morphology, while ORI-GC-NP had a rotiform shape. The apparent increase of particle size and the rotiform shape of ORI-GC-NP compared with ORI-NP provided an evidence of the coating of GC polymers to the oily cores in nanoparticles.

Figure 2-D illustrates the *in vitro* release profiles of

ORI-GC-NP in pH 7.4 (microenvironment) and 6.8 (tumor cell environment) buffers. Results shown that the release properties of oridonin from ORI-GC-NP fit to a two-stage exponential kinetic model with a fast release at first and a slower sustained release followed. The cumulative release rate of oridonin from ORI-GC-NP was 72.7% at pH 7.4, while 97.6% at pH 6.0. The slight pH dependence might be attributed to the coating of GC on NPs, which contributes to more drugs releasing from NPs in tumor cells.

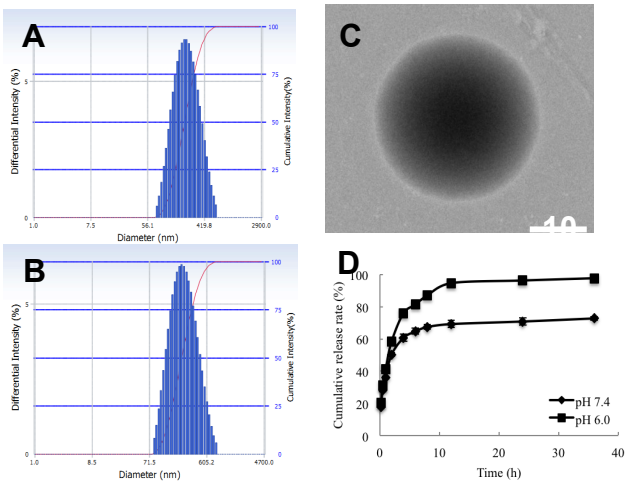

Figure 2. The size distribution and morphology of drug-loaded nanoparticles: (A) size distribution of ORI-NP, (B) size distribution of ORI-GC-NP, (C) morphology of ORI-GC-NP, (D) *in vitro* oridonin release profiles in pH 7.4 and 6.8.

Cytotoxicity of blank nanoparticles

As cationic polymers could aggregate on cell surfaces and display critical intracellular processes, cytotoxicity of the GC polymers may interfere the antitumor activity of ORI-GC-NP [16]. To exclude the interference of polymers, the cytotoxicity of nanoparticles without ORI against HepG2 and MCF-7 cells was measured by MTT assay. Figure 3 showed that cell viability rate remained stable at more than 80% as the concentration of blank nanoparticles increased[17], which indicated that blank nanoparticles have no significant toxicity on HepG2 and MCF-7 cells.

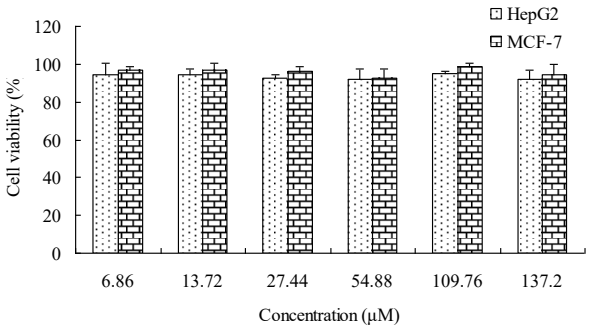

Figure 3. Cytotoxic effects of blank nanoparticles on HepG2 cells and MCF-7 cells for 72 h treatment. Data were expressed as the mean ± SD (n = 4).

In vitro antitumor activity test of drug-loaded nanoparticles

For further investigation of the potential therapeutic efficacy of drug-loaded nanoparticles, HepG2 and MCF-7 cells were treated with ORI solution, ORI-NP and ORI-GC-NP at different ORI concentrations ranging from 13.72 to 109.76 μM for 24, 48 and 72 h, respectively. MCF-7 cells, without asialoglycoprotein receptors on the surface, were used as control to confirm that galactose decorated nanoparticles were taken up by HepG2 cells via the receptor-mediated mechanism. Figure 4 displayed the *in vitro* antitumor activity of ORI-GC-NP, ORI-NP and ORI solution against HepG2 and MCF-7 cells. As shown in Figure 4, significantly higher cytotoxicity was found in cells exposed to ORI-loaded nanoparticles than free ORI for the same time. Otherwise, as drug concentration increased and action time of the drug prolonged, cell viability of HepG2 and MCF-7 decreased. That is to say, the antitumor activity of drug-loaded nanoparticles and ORI solutions against HepG2 and MCF-7 cells increased in a concentration and time dependent manner.

Meanwhile, the antitumor activities of ORI-GC-NP, ORI-NP, and ORI solution were evaluated by the IC_{50} (half maximal inhibitory concentration) values. Table 1 and Table 2 showed the IC_{50} values of three formulations against HepG2 and MCF-7 cells, respectively. Table 1 suggested that the IC_{50} values of ORI-GC-NP were lower than that of ORI-NP and

ORI solution, indicating that ORI-GC-NP could significantly improve the antitumor activity of oridonin against HepG2 cells. Additionally, in the case of HepG2, IC_{50} values of ORI-GC-NP were 47.09, 29.32 and 26.59 μM after incubated for 24, 48 and 72 h, respectively. By comparison, in Table 2, IC_{50} values of ORI-GC-NP against MCF-7 cells were 54.87, 32.97 and 31.07 μM, respectively. The data suggested that ORI-GC-NP showed more effective antitumor activity against HepG2 cells than MCF-7, owing to the increased uptake of the nanoparticles via the receptor-mediated mechanism [17, 18]. Apart from these, for ORI-NP, drug-loaded nanoparticles without galactosylation, the IC_{50} values were 56.04, 39.40 and 31.63 μM for 24, 48 and 72 h against HepG2, while 47.25, 30.03 and 27.83 μM against MCF-7 cells. For ORI solution, the IC_{50} values were 74.26, 48.93 and 43.68 μM for 24, 48 and 72 h against HepG2, while 67.49, 45.61 and 36.72 μM against MCF-7 cells. The data indicated that the inhibition rates of ORI-NP and ORI solution against HepG2 were lower than MCF-7 cells, which might due to that the sensitive degrees of these two tumor cells to ORI were different. Taken together, the order of the antitumor activity of the three formulations against HepG2 cells were ORI-GC -NP > ORI-NP > ORI solutions, resulting from the increasing targeting of oridonin nanoparticles decorated with galactosylated chitosan to HepG2 cells, whereas that the order against MCF-7 were ORI-NP > ORI-GC-NP > ORI solutions, related to the enhanced internalization of ORI-NP with a relatively smaller particle size via endocytosis or phagocytosis.

Table 1. The IC50 values of ORI-loaded nanoparticles and ORI-solution on HepG2.

	ORI-GC-NP			ORI-NP			ORI solution		
Time(h)	24	48	72	24	48	72	24	48	72
IC50(μM)	47.09	29.32	26.59	56.04	39.40	31.63	74.26	48.93	43.68

Table 2. The IC50 values of ORI-loaded nanoparticles and ORI-solution on MCF-7.

	ORI-GC-NP			ORI-NP			ORI solution		
Time(h)	24	48	72	24	48	72	24	48	72
IC50(μM)	54.87	32.97	31.07	47.25	30.03	27.83	67.49	45.61	36.72

Observation of cell morphology

To further confirm the increasing antitumor activity of ORI-GC-NP compared with ORI-NP and ORI solution, the changes in cellular morphology were investigated using a reverse fluorescence microscopy. Figure 5 showed the morphological images of HepG2 and MCF-7 cells treated with different samples after 24 h at the same conditions. The untreated cells for control were polygonal with clear cellular skeletons (Figure 5A-B), whereas the morphological changes were observed in Figure 5C-H, including cell shrinkage and rounding after 24 h culture with all of the three formulations. In addition, the number of normal HepG2 cells in ORI-GC-NP was lower than in ORI-NP and ORI solution, while the number of MCF-7 cells in ORI -NP was lower than in ORI-GC-NP and ORI solution. These results agreed with the conclusions obtained from the previous experiments of *in vitro* antitumor activity test of drug-loaded nanoparticles.

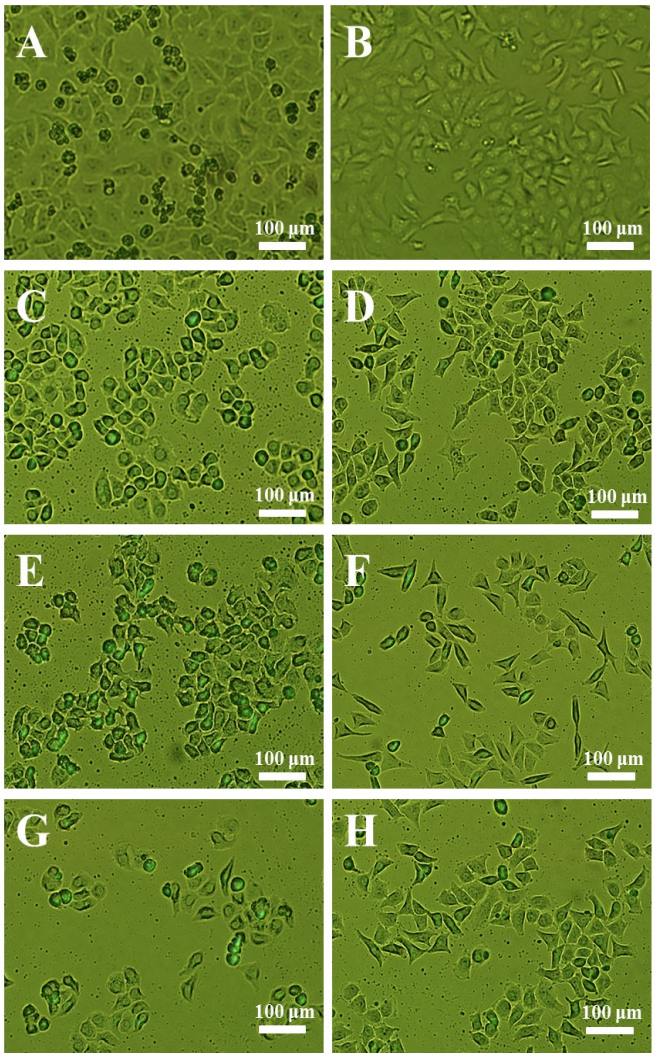

Figure 5. Cellular morphologies of HepG2 and MCF-7 cells with different treatments: (A) untreated HepG2 cells, (B) untreated MCF-7 cells, (C) ORI solution against HepG2, (D) ORI solution against MCF-7, (E) ORI-NP against HepG2, (F) ORI-NP against MCF-7, (G) ORI-GC-NP against HepG2, (H) ORI-GC-NP against MCF-7.

CONCLUSIONS

This study chose GC-coated nanoparticles as an active hepatocyte-targeted delivery system for ORI, and the nanoparticles was successfully prepared and characterized with uncoated nanoparticles as control. Based on the result that blank nanoparticles without ORI exhibits no cytotoxicity, MTT assay and morphological changes suggested that ORI-GC-NP exhibited an enhanced anticancer activity against HepG2 cells compared with both ORI-NP and ORI solution. However, distinct phenomena were observed for MCF-7 cells at the same conditions. The determinations revealed that galactose could enhance the uptake through the mechanism of galactose-specific receptor-mediated endocytosis, and cytotoxic ability of ORI-loaded nanoparticles to HepG2 cells increased in a concentration and time dependent manner. In coclusion, the modified nanoparticles coated with galactosylated chitosan would be promising carriers for specific delivery into liver cancer cells.

ACKNOWLEDGEMENTS

This work was supported by Key Research and Development Plan Project of Shandong Province, China. The programme number is 2016GSF202010.

Conflicts of interest

The authors report no conflicts of interest.

REFERENCES

[1] A.S. Lorenza Rimassa, The present and the future landscape of treatment of advanced hepatocellular carcinoma, Digestive and Liver Disease, 42S (2010) S273–S280. 60516-6 View Article

[2] A.-L.C. Jacqueline Whang-Peng, Chiun Hsu, Chien-Ming Chen, Clinical Development and Future Direction for the Treatment of Hepatocellular Carcinoma, J Exp Clin Med, 2 (2010) 93–103. 60016-2 View Article

[3] C.Y. Li, E.Q. Wang, Y. Cheng, J.K. Bao, Oridonin: An active diterpenoid targeting cell cycle arrest, apoptotic and autophagic pathways for cancer therapeutics, Int J Biochem Cell Biol, 43 (2011) 701-704. PMid:21295154 View Article PubMed/NCBI

[4] H. Wang, Y. Ye, S.Y. Pan, G.Y. Zhu, Y.W. Li, D.W. Fong, Z.L. Yu, Proteomic identification of proteins involved in the anticancer activities of oridonin in HepG2 cells, Phytomedicine, 18 (2011) 163-169. PMid:20724128 View Article PubMed/NCBI

[5] M. Cheng, Q. Li, T. Wan, X. Hong, H. Chen, B. He, Z. Cheng, H. Xu, T. Ye, B. Zha, J. Wu, R. Zhou, Synthesis and efficient hepatocyte targeting of galactosylated chitosan as a gene

carrier in vitro and in vivo, J Biomed Mater Res B Appl Biomater, 99 (2011) 70-80. PMid:21656667 View Article PubMed/NCBI

[6] R. Rohilla, T. Garg, A.K. Goyal, G. Rath, Herbal and polymeric approaches for liver-targeting drug delivery: novel strategies and their significance, Drug Deliv, 23 (2016) 1645-1661. PMid:25101832

[7] W.J. Lin, T.D. Chen, C.-W. Liu, Synthesis and characterization of lactobionic acid grafted pegylated chitosan and nanoparticle complex application, Polymer, 50 (2009) 4166-4174. View Article

[8] M.J. Santander-Ortega, J.M. Peula-Garcia, F.M. Goycoolea, J.L. Ortega-Vinuesa, Chitosan nanocapsules: Effect of chitosan molecular weight and acetylation degree on electrokinetic behaviour and colloidal stability, Colloids Surf B Biointerfaces, 82 (2011) 571-580. PMid:21071187 View Article PubMed/NCBI

[9] F. Sonvico, A. Cagnani, A. Rossi, S. Motta, M.T. Di Bari, F. Cavatorta, M.J. Alonso, A. Deriu, P. Colombo, Formation of self-organized nanoparticles by lecithin/chitosan ionic interaction, Int J Pharm, 324 (2006) 67-73. PMid:16973314 View Article PubMed/NCBI

[10] A.A. D'Souza, P.V. Devarajan, Asialoglycoprotein receptor mediated hepatocyte targeting - strategies and applications, J Control Release, 203 (2015) 126-139. PMid:25701309 View Article PubMed/NCBI

[11] V.B. Cattani, L.A. Fiel, A. Jager, E. Jager, L.M. Colome, F. Uchoa, V. Stefani, T. Dalla Costa, S.S. Guterres, A.R. Pohlmann, Lipid-core nanocapsules restrained the indomethacin ethyl ester hydrolysis in the gastrointestinal lumen and wall acting as mucoadhesive reservoirs, Eur J Pharm Sci, 39 (2010) 116-124. PMid:19932749 View Article PubMed/NCBI

[12] C. He, Y. Hu, L. Yin, C. Tang, C. Yin, Effects of particle size and surface charge on cellular uptake and biodistribution of polymeric nanoparticles, Biomaterials, 31 (2010) 3657-3666. PMid:20138662 View Article PubMed/NCBI

[13] A.K. Iyer, G. Khaled, J. Fang, H. Maeda, Exploiting the enhanced permeability and retention effect for tumor targeting, Drug Discov Today, 11 (2006) 812-818. PMid:16935749 View Article PubMed/NCBI

[14] J.W. H. Maeda, T. Sawa, Y. Matsumura, K. Hori, Tumor vascular permeability and the EPR effect in macromolecular therapeutics_ a review, Journal of Controlled Release 65 (2000) 271–284. 00248-5 View Article

[15] J.B. Liu, J.Y. Yue, Preliminary study on the mechanism of oridonin-induced apoptosis in human squamous cell oesophageal carcinoma cell line EC9706, J Int Med Res, 42 (2014) 984-992. PMid:24874012 View Article PubMed/NCBI

[16] G.S. Kokhou Wong, Xueqing Zhang, Hui Dai, Ye Liu, Chaobin He, Kam W. Leong, PEI-g-chitosan, a Novel Gene Delivery System with Transfection Efficiency Comparable to Polyethylenimine in Vitro and after Liver Administration in Vivo, Bioconjugate Chem., 17 (2006) 152−158. PMid:16417264 View Article PubMed/NCBI

[17] R. Yang, F. Meng, S. Ma, F. Huang, H. Liu, Z. Zhong, Galactose-decorated cross-linked biodegradable poly(ethylene glycol)-b-poly(epsilon-caprolactone) block copolymer micelles for enhanced hepatoma-targeting delivery of paclitaxel, Biomacromolecules, 12 (2011) 3047-3055. PMid:21726090 View Article PubMed/NCBI

[18] K. Na, E. Seong Lee, Y.H. Bae, Adriamycin loaded pullulan acetate/sulfonamide conjugate nanoparticles responding to tumor pH: pH-dependent cell interaction, internalization and cytotoxicity in vitro, Journal of Controlled Release, 87 (2003) 3-13. 00345-0 View Article